

Rutgers 12-Inch Cyclotron Electrostatic Deflector

Timothy W. Koeth, Timothy S. Ponter, Daniel E. Hoffman, William S. Schneider, James E. Krutzler
Rutgers University, Piscataway, NJ, 08854

ABSTRACT The Rutgers 12-Inch Cyclotron is a 1.2 MeV particle accelerator dedicated to beam physics instruction and accelerator component research and development. Previous publications by the Rutgers Cyclotron group have described observed axial betatron motion, which was found to be consistent with radially increasing energetic protons [1,2]. However, irrefutable verification of the final beam energy required a spectrometer based measurement. An internal $E \times B$ spectrometer, a variant on the Wien Filter, was chosen as to utilize the existing magnetic field. This Wien Filter also served as a prototype extraction channel for our 19-Inch Cyclotron project currently under construction. This paper reviews the theory of the Wien Filter and its specific application to our accelerator, details our apparatus, and reports on initial measurements with beam.

INTRODUCTION Large amplitude axial (vertical) betatron motion has been observed in the Rutgers 12-Inch Cyclotron. The measured axial phase advancement per revolution was measured at several radii. The phase advancement was shown to strongly agree with theoretical expectations of a beam of implied energy circulating at a given radii with our known magnetic field and field gradient.

Since various internal target experiments rely on a radial intercept to select the incident beam energy, it was deemed prudent to perform an absolute beam energy measurement at a minimum of one fixed radii.

A thin, curved, grounded sheet formed the septum and separates the main accelerating volume and the deflection channel. A slightly greater curved high voltage (HV) electrode was concentrically arranged to complete the deflection channel with an average 0.31 inch gap spacing. The deflector tangentially intercepted the spiraling cyclotron beam at a radius of 4.0 inches and transported the beam to a radius of 4.5 inches in 43° of azimuth.

The deflection channel had a nominal radius of curvature of 7 inches. Since this was much larger than the entering ion's radius of curvature of 4 inches, ions that entered the un-energized channel would impinge on the septum and quickly be lost, certainly unable to traverse the length of the channel. High voltage (HV) applied to the electrode generates a deflecting transverse electric field. Only an appropriate negative electric field will partially negate the magnetic field's bending force permitting the successful transmission of ions. A greater field will cause the ions to terminate on the deflector

and be lost, and a lesser field will cause the ions to terminate on the septum, only ions of the correct q/m ratio and velocity will be permitted completely through the channel to be successfully detected. Thus the channel acts as a velocity filter, also known as a Wien Filter, enabling measurements of an ion beams central energy and energy spread.

WIEN FILTER THEORY A Wien Filter utilizes a set of orthogonal magnetic and electric fields to act as a velocity filter for ions of a specified q/m ratio. The Lorentz force on a particle of charge q with mass m traveling at a velocity v is:

$$\vec{F} = \frac{d\vec{p}}{dt} = m \frac{d\vec{v}}{dt} = q(\vec{E} + \vec{v} \times \vec{B})$$

For a particle of charge to mass ratio of q/m and velocity v to go un-deflected (i.e. $dv_{\perp}/dt = 0$) through a channel with transverse and orthogonal \mathbf{E} and \mathbf{B} fields, the net Lorentz force has to be zero:

$$0 = \frac{q}{m} (\vec{E} + \vec{v} \times \vec{B})$$

$$(\vec{E} + \vec{v} \times \vec{B}) = 0$$

Considering all orthogonal fields and motion, we drop the vector notation and re-arrange the above to solve for the ratio of E to B to permit any ion of velocity v

$$v = -E/B,$$

with charge to mass ratio of q/m . The simplest example is a proton, ${}_1\text{H}^+$, with a single unit charge and single atomic mass unit. Next, fully ionized deuterium has a q/m of $1/2$, ${}_2\text{H}^+$. However, so does helium, ${}_4\text{He}^{++}$. This creates an

ambiguity which cannot be resolved by the Wien Filter.

It might be expected that the combined effect of the cyclotron's resonant acceleration and our embedded Wien Filter's velocity selection might separate the mass ambiguity. However, this is not the case, as the cyclotron itself acts a velocity filter at each of its radii. From the most fundamental cyclotron equation, one can see that the ion revolution frequency is dependent on ion's charge to mass ratio:

$$f_{cyc} = \frac{B}{2\pi} \frac{q}{m}$$

Thus, for a fixed magnetic field, the resonant 'cyclotron' frequency remains the same for both ionized deuterium, ${}^2\text{H}^+$, and fully ionized helium ${}^4\text{He}^{++}$. It also holds that at any given radius, both the deuterium and helium cover the same angular distance and thus must have the same angular velocity to keep in step with the oscillating RF voltage. Now it is easily seen that the velocity of either deuterium or helium will be the same at the entrance to the deflection channel. Note, while the two ions have the same velocity, they obviously do not have the same energy.

Our application of the E×B velocity filter is a variant of the Wien Filter, as it does not completely straighten the orbit, rather the beam still follows an arc, one with an increased orbit curvature. Thus, the analysis is not as simple as the electric force canceling the magnetic force.

In our 12-inch cyclotron, the resonant beam is tangentially intercepted at a radius of 4 inches (0.1016 m) where the initial (ρ_0), or undeflected, orbit's radius of curvature is increased from 4.0 inches to the new, or deflected orbit curvature (ρ_1), of 7.0 inches (0.18 m).

The following is a general derivation for the required deflector electrode voltage, and is followed with a numerical example with protons. Relating the centripetal force to the Lorentz Force we write:

$$\vec{F} = \frac{mv^2}{\rho} = q(\vec{E} + \vec{v} \times \vec{B})$$

Where is ρ the bending radius. Again assuming orthogonal fields and velocity, solve for the reciprocal of radius in the generic case of both E- and B-fields.

$$\frac{1}{\rho} = \frac{q}{mv^2} (E + vB)$$

Of course, the normal cyclotron orbit condition is free of any E-field, so the specific reciprocal of radius of curvature is just:

$$\frac{1}{\rho_0} = \frac{qvB}{mv^2}$$

And with the transverse electric field applied, the new reciprocal of radius of curvature is:

$$\frac{1}{\rho_1} = \frac{qE}{mv^2} + \frac{qvB}{mv^2}$$

Take the reciprocal difference between the two instances:

$$\frac{1}{\rho_1} - \frac{1}{\rho_0} = \frac{qE}{mv^2} + \frac{qvB}{mv^2} - \frac{qvB}{mv^2}$$

Obviously the two right most terms cancel, and finally solving for the electric field we have:

$$E = \frac{mv^2}{q} \left(\frac{1}{\rho_1} - \frac{1}{\rho_0} \right)$$

Note that in the non-relativistic case, the mv^2 term is just twice the ion's kinetic energy. Substituting the non-relativistic cyclotron kinetic energy condition,

$$T = \frac{q^2 B^2 \rho^2}{2m}$$

and keeping in mind that $\rho = \rho_0$ at the point of interception, we can re-write the equation for the electric field as:

$$E = \frac{2T}{q} \left(\frac{1}{\rho_1} - \frac{1}{\rho_0} \right) = \frac{qB^2 \rho_0^2}{m} \left(\frac{1}{\rho_1} - \frac{1}{\rho_0} \right)$$

This determines the necessary electric field; we must multiply the electric field by the HV electrode-septum gap spacing to determine the required applied potential.

Using the values of ρ_0 and ρ_1 listed above, we find that for protons in a 1.0 Tesla magnetic field, a transverse electric field of 4.2 MV/m is required. The nominal electrode-septum spacing is 0.31 inches, thereby setting the electrode voltage at 33 kV.

HARDWARE The deflector installation consists of three major components, the deflector assembly, the phosphor screen detector, and the high voltage power supply. Each aspect of the deflection system has key features and difficulties which are separately discussed below.

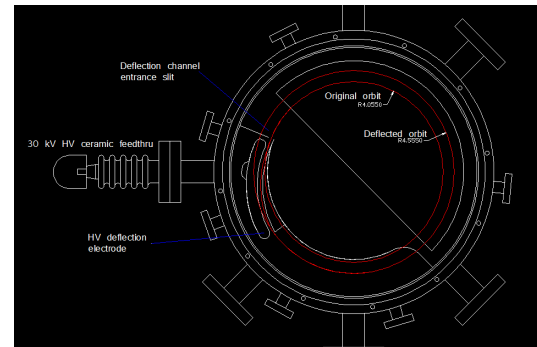


Figure 1. Early mechanical drawing indicating placement of deflector wrt to ion orbits.

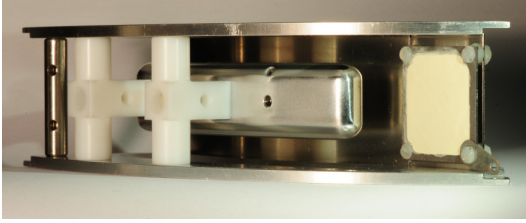


Figure 2. “Upstream” view from target end of assembled deflector. Note isolated phosphor plate.

Deflector Assembly The deflection channel was constructed as a modular assembly that could easily be removed from and replaced within the cyclotron chamber, as shown in Figure 2. Two aluminum plates separated by stainless steel posts formed the skeletal structure. The septum’s curve was machined as a stepped shelf along the inside edge of the top and bottom structural plates. A thin (0.005 inch thick) stainless steel strip was seated against the step forming the septum. Thin strips of aluminum matching the septum’s curvature were bolted onto the shelf clamping the septum in place and holding its curvature – see Figure 3.



Figure 3. Partially disassembled deflector.

The high voltage electrode was machined 3/8 inch thick from 7075 aluminum; each corner was rounded with a radius also of 3/8 inch. The curvature of 3/8-inch was based on the anticipated voltage, including a significant margin of error. The electric field resulting from a curved metallic surface follows

$$E_{\max} = \frac{0.9V}{r \ln\left(\frac{r+a}{r}\right)}$$

Where r is the radius of the curved surface, and a is the distance of the closest approach, limiting E_{\max} to a conservative 170 kV/inch. In addition, the electrode was highly polished. It was supported from the back by stem of two T-shaped Teflon insulators. Bosses were machined in the tips of each arm of the T-insulators, the

bosses were seated in detents in top and bottom plates. The T-insulator stems were deeply counter-bored and finished with a blank through hole. Two tapped holes on the rear of the HV electrode, and Nylon screws secured the electrode to the base of the T-insulators, which can be seen in place in Figures 3 and 4.

Electrical connection was made to the HV electrode by directly seating a HV ceramic vacuum feed-through conductor into a third and final clearance hole in the back of the electrode, and is captured by a set screw.

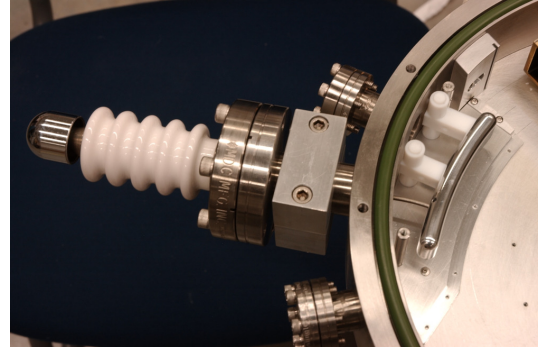


Figure 4. HV vacuum feed through and connection to the electrode (deflector housing and septum removed for photo).

After initial operation, internal arcing between the HV electrode and the grounded housing clearly indicated secondary electron emission. The evidence was in pitting, shown in Figure 4 on the internal surfaces of the top and bottom structural plates - the bulk of which occurred directly above and below the perimeter of the HV electrode. A general rule-of-thumb places the threshold for damage from arcing at 1 Joule. Locations of the closest approach, such as directly below the centerline did not show much pitting, exonerating field emission based brake-down. Further, damage was only noted on the top and bottom plates, not the deflector electrode, suggesting secondary electrons were emitted on the electrode, accelerated away from the HV electrode, tightly following the vertical magnetic field lines.

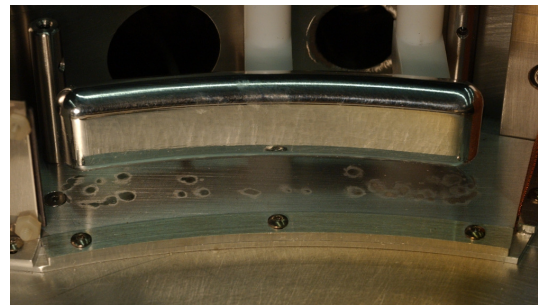


Figure 5. Pitting observed from arcing.

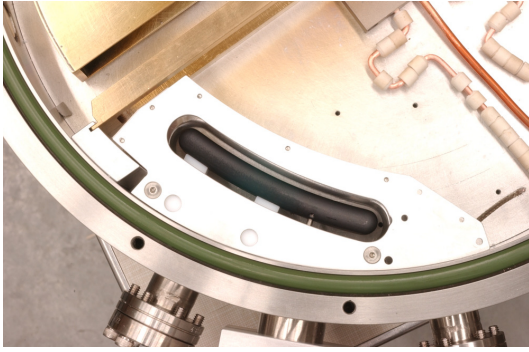


Figure 6. Deflector assembly, with clearance slot exposing electrode, coated with Aerodag-G.

Several steps were taken to mitigate the arcing. First, the polished HV electrode was coated with Aerodag-G graphite lubricant to reduce the coefficient of secondary electron emission. Three thin coatings of Aerodag-G were applied from an aerosol dispenser using an alcohol based propellant. The coated electrode was then baked at 125° C for 1 hour in standard atmosphere. Care was taken in handling the electrode as not to scrape the coating. However, from the handling it did receive, the coating was found to be surprisingly robust.

Secondly, a clearance slot parallel to the deflection electrode was machined into the top and bottom structural plates which, shown in Figure 6, was intended to further reduce the electric field between them.

Phosphor Screen Observation of the initial beam transported through the deflection channel was viewed impinging upon a phosphor screen located at the exit. The screen was mounted at a 45° angle with respect to the incident beam and to the axis of a glass view port. Due to the extremely small geometry and cost of custom manufactured phosphor screens, we elected to produce our own screens. Mastering this technique has proven invaluable, allowing experiments with many different phosphors and target arrangements.

It should be possible with fast phosphors in conjunction with either photomultiplier tubes or gated cameras to time resolve the beam structure. Initially phosphor type P-22 green, the standard oscilloscope CRT phosphor, was used for maximum visual sensitivity. Using a settling technique, 1-inch square metal plates were coated with a uniform phosphor layer. The phosphor coated plate was attached to a metal carrier plate using electrically insulating screws – the phosphor plate was separated from the carrier plate by 1/8-inch to keep the capacitance reasonably low. The carrier plate was clamped into the deflector assembly in a manner similar

to the mounting of the septum. The center conductor of a coaxial cable was connected to the phosphor plate and the coax shield to the grounded carrier plate, the cable was routed to a BNC vacuum feed through connector. The electrical isolation and connectivity permits the phosphor plate to double as a Faraday collector. The low capacitance of the collecting plate should permit time-resolved electrical measurements of the impinging beam.

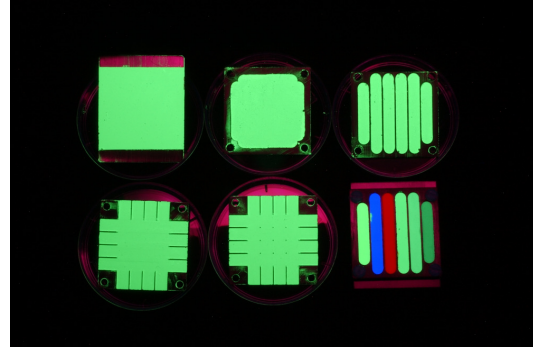


Figure 7. Various Rutgers Cyclotron phosphor screen target arrangements. Including, left to right (top row) a directly coated carrier plate, the remainder are on isolation plates, solid plate, six identical strips, (bottom row) edge fiducial markings, edge and central fiducial markings, and finally test strips with six different phosphors.



Figure 8. Image of the phosphor plate with edges populated with fiducial markings.

High Voltage Power As seen above, a potential of 33 kV is required on the electrode to produce a transverse electric field of 4.2 MV/m. Initially only a constant-voltage regulated 30 kV power supply was available. For safety, the supply required a current limiting series resistor of 75 MΩ in the event of a short or arc. Even though the supply was capable of providing 30 kV, the leakage current from corona reduced the maximum achievable deflector electrode voltage to 28 kV. Even so, 28 kV was sufficient to just bring the beam to the edge of the screen, as seen in Figure 10.

Subsequently, a surplus Bertan 205A-50N 50 kV power supply was ordered and installed. This supply was also only a constant voltage supply requiring a 150 M Ω current limiting resistor. The resistor was housed in an acrylic tube, capped at both ends, which was then externally covered with a grounded copper mesh. The resistor housing was installed in a relatively inaccessible location at the top and backside of the magnet yoke.

The high voltage was brought from the supply to the series resistor, and continued from the resistor to the cyclotron chamber's HV vacuum bushing using portable x-ray machine "Mammoflex" coaxial cable. The Mammoflex cable is rated for 60 kV and had a capacitance of 56 pF per foot. After installation of the new supply and cable, mysterious behavior was noticed and is still not fully explained. At sufficiently high voltages (~ 30kV) arcing inside the chamber occurred – both light and audible snapping were observed. Coincident with the internal arcing, external arcing was observed between the shield of the Mammoflex cable (of the 6 foot segment between the resistor and chamber) and chassis ground, such as the magnet frame. One such arc terminated on the upper magnet coil, causing the magnet power permanent damage, requiring costly repair. The stored energy in the 6 foot cable at 30 kV is about 0.2 Joules, not much lower than the rule-of-thumb damage threshold of 1 Joule. It is also known that the focusing influence of the magnetic field can enhance the damage of an electrical discharge.

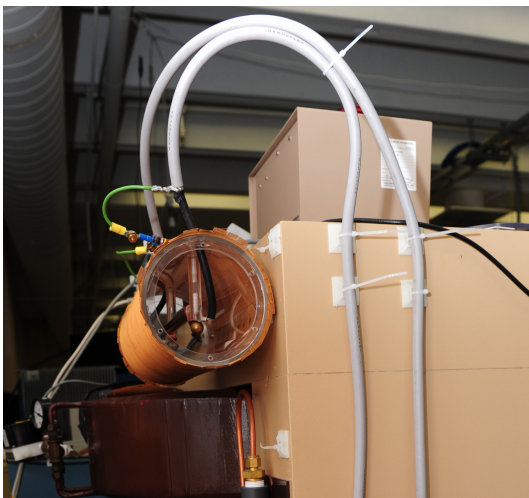


Figure 9. 150 M Ω HV resistor installation (end cap removed to expose resistor for photo), note two 68 Ω resistors in series with HV cable shields – arcing was observed between the green wire and copper mesh, bypassing the 68 Ω resistor.

After consulting an experienced high voltage engineer, it was suggested that due to the rapid formation of the internal arc, the segment of HV cable between the resistor and chamber was effectively a Blumlein HV pulse generator [5], several steps were taken to suppress the arcing. First, the HV cable length was reduced to the bare minimum required, thereby minimizing the stored energy in the cable. To limit the discharge current, 68 Ω , 2 Watt carbon resistors were placed in series with the cable shield at the resistor box. However, streamers traveling greater than 1 inch in air were still observed bypassing the 68 Ω resistors. The resistors were subsequently tested and found to be undamaged and properly functioning.

A 5 M Ω HV resistor was then next installed in series with the center conductor and the chamber just prior to the HV vacuum chamber bushing. This has been found to suppress the arcing. Finally, to ensure machine safety, the HV coaxial cables have been routed clear of any sensitive electronics in the event of a reoccurrence.

An IEEE-488C GPIB interface has been purchased for the Bertan HV 205A-50N power supply, enabling remote computer control. There is a planned project to automate the sweeping of the cyclotron magnetic field and HV deflector while recording the beam current, effectively turning the cyclotron into a very sensitive accelerator based q/m spectrometer.

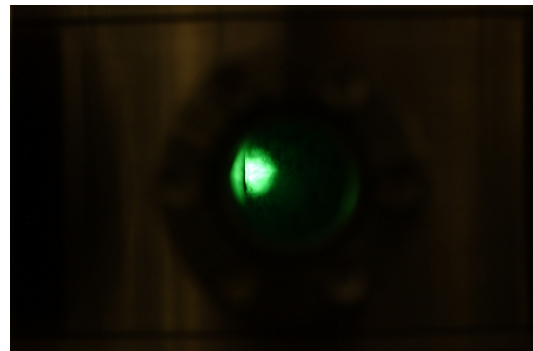


Figure 10. First image of 500 keV protons on phosphor screen.

MEASUREMENTS Initial beam measurements were performed with the cyclotron operating at an RF frequency of 14.900 MHz at 400 watts input power and magnetic field of approximately 1 Tesla (the magnetic field is adjusted for maximum beam current on the original adjustable faraday collector). Once beam was established, the adjustable faraday collector was fully retracted, allowing the accelerated beam to encounter the entrance slit of the deflection channel. The deflector HV supply was slowly ramped while observing the phosphor screen. A

clearly visible green spot appeared on the left most edge of the phosphor screen, and continued to move towards the right with increased HV until the maximum limit of the power supply was reached. Again, although the power supply was capable of supplying 30 kV, the maximum achievable voltage on the HV deflection electrode was about 28 kV due to the voltage drop across the series resistor. This was the first observation of a deflected beam in the 12-Inch Cyclotron.

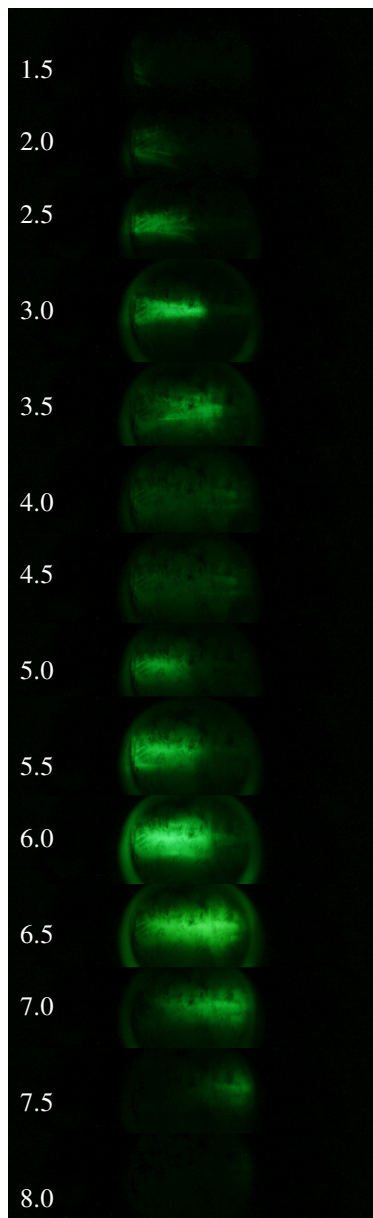


Figure 11. A photo sequence of the cyclotron in operation, stepping through voltages on deflector in 0.5 kV steps (numeric labels).

The magnetic field was then approximately halved, 0.44 Tesla, and the measurements repeated. The RF frequency was held fixed at

14.900 MHz. The deflector voltage was stepped in 0.5 kV increments and a photograph of the phosphor screen was taken. Vertically stitching the sequence of images reveals the admittance of two different ions. Given the deflector voltage and magnetic field strength, the q/m values were determined.

Accounting for the deflection voltage, analysis of the lower beam spot, centered at 6.0 kV, shows a q/m of 1.0 – the signature of a proton, H^+ . However, the cyclotron frequency at 0.44 T for H^+ is 6.71 MHz, and the operating frequency was 14.900 MHz, yielding a harmonic number of 2.22. This result is not understood, as only integer odd harmonic numbers support magnetic resonance acceleration. At an even harmonic, when acceleration occurs at a gap crossing, deceleration must occur at the subsequent crossing, yielding zero net accelerator per revolution. In the region between an even and odd harmonic, there is a balance of acceleration and phase slippage which the ions encounter. Operating a cyclotron near, but not on, an odd harmonic, can still lead to a successful resonantly accelerated beam, provided that the integrated phase slippage over all revolutions is less than 180 before hitting the target or extraction point. The greater the DEE voltage, the fewer the number of ion revolutions are needed to achieve the desired energy, thus the tolerance of phase slippage per turn increases with DEE voltage. Our case was modeled in SIMION, however no DEE voltage was found to successfully bring protons from the ions source to the deflector operating at the harmonic of 2.22.

A similar analysis was performed for the peak observed at 3.0 kV, corresponding to an ion with q/m of $1/2$, such as ${}^2H^+$ or ${}^4He^{++}$. The rotational cyclotron frequency for q/m of $1/2$ is 3.5 MHz while the driving a frequency was 14.900 MHz, yielding a harmonic number of 4.25, again this is not understood and is receiving further investigation.

ENERGY RESOLUTION Several factors contribute to the cyclotron beam's energy spread at any given radius, such as the finite acceptance of ions during an rf cycle leading to a spectrum of radial betatron amplitudes, as well as the transverse spot size becoming comparable to the radial turn-to-turn spacing at the deflector. The ideal deflection channel would admit particles of a single energy; however this is impractical, as very few ions would be at that actual energy, thus discarding most of the ion beam. As such the deflector must admit ions over a range of energies at the cost of energy selectivity, or

resolution. This is accomplished through a finite width entrance slit at the. A future cyclotron-student project to perform a thorough analysis of the deflector and its optics properties; this will include flying ions in a full 3D simulation.

However, for a preliminary estimation of the deflector's resolution, we calculate the acceptable spread in ion energies that are admitted through an infinitely thin gap centered on the entrance slit, see Figure 12. We assume the ions are tangentially incident, and do not consider an incoming angular offset.

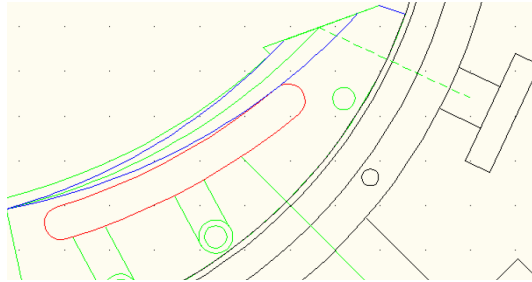


Figure 12. Deflector layout showing width of ion beam (blue curves) solely due to energy spread admitted from a single point.

First, we can solve for the energy of the ideal ion, following the centerline trajectory through the deflection channel:

$$T_{nom} = \frac{V\rho}{2d} \left(1 + \frac{\rho}{\Delta\rho} \right)$$

where d is the high voltage gap spacing, ρ is the radius of interception $\Delta\rho$ is the increase in curvature, such that $\rho + \Delta\rho$ is the new bending radius in the deflector. It can be easily seen that an ion of slightly lower energy than the ideal, ε^- , can map out an arc with larger curvature, $\Delta\rho + \varepsilon_r^-$, but still successfully exit the deflection channel:

$$T_- = \frac{V\rho}{2d} \left(1 + \frac{\rho}{\Delta\rho + \varepsilon_r^-} \right)$$

Similarly, we can write for an ion of slightly greater energy than nominal, ε^+ , has a smaller radius of curvature, $\Delta\rho - \varepsilon_r^+$:

$$T_+ = \frac{V\rho}{2d} \left(1 + \frac{\rho}{\Delta\rho - \varepsilon_r^+} \right)$$

By subtracting the above equation from the previous, we arrive at a band of energies that are permitted through the channel:

$$\Delta T = T_+ - T_- = \frac{V\rho^2}{2d} \left(1 + \frac{\varepsilon_r}{\Delta\rho^2 - \varepsilon_r^2} \right)$$

For the 12-Inch Cyclotron values, $V=28$ kV, $\rho=4.125$ inches, $d=0.31$ inches, $\Delta\rho=2.757$

inches, $\varepsilon_r=0.118$ inches, we arrive at a $\Delta T=25$ keV for a nominal 500 keV proton beam, a 5%.

The resolution will be worse than this figure, as the entire entrance slit is admitting ions, which may have an angular component as well. These effects will be thoroughly studied in a future deflector document.

FUTURE DESIGN A scaled version of the of the 12-Inch Cyclotron's deflector will be the basis of the 19-Inch cyclotron deflection system. The 19-Inch cyclotron projects has a design constraint limiting the HV potential to 50 kV as a second 50 kV Bertan supply has been purchased. The stated goal is to extract and transport the 19-Inch Cyclotron's beam to a diagnostic and experimental chamber. As such, the extracted beam will need to traverse the rapidly falling vertical fringe field. The 19-Inch extraction design will incorporate an increase the deflection channel's gap, reducing the extraction field, through the region of declining magnetic field.

CONCLUSION A high-voltage electrostatic beam deflection channel has been designed, constructed, and commissioned in the Rutgers 12-Inch cyclotron. A 500 keV proton beam has successfully been intercepted at it's nominal cyclotron radius of 4.0 inches and brought a radius of 4.5 inches in 43° of azimuth. This project has provided the experience necessary to confidently design an extraction channel for the 19-Inch cyclotron project.

ACKNOWLEDGEMENTS. The authors thank Prof. M. Kalelkar for arranging the needed funding to make this work possible. We are also indebted to the Rutgers Machine shop for their support, and to Heidi Baumgartner for assistance during the deflector installation. Finally, we thank Chris Jensen of Fermi National Accelerator for his many reviews, discussions, and suggestions leading to a stable high voltage delivery system.

REFERENCES

- [1] http://www.physics.rutgers.edu/cyclotron/papers/Betatron_Studies.pdf
- [2] http://www.physics.rutgers.edu/cyclotron/papers/IonSourceStudiesII_march_26_2008.pdf
- [3] J.J. Livingood, "Principles of Cyclic Particle Accelerators," D. Van Nostrand, 1961
- [4] H. Wollnik, "Optics of Charged Particles" Academic Press, 1987
- [5] C. Jensen, Fermi National Accelerator Lab, private communication